ACS OMEGA

Open Access

http://pubs.acs.org/journal/acsodf

Article

Revealing the DNA Binding Modes of CsoR by EPR Spectroscopy

Yasmin Igbaria-Jaber, Lukas Hofmann, Lada Gevorkyan-Airapetov, Yulia Shenberger, and Sharon Ruthstein*

Cite This: *ACS Omega* 2023, 8, 39886−39895

Read Online

ACCESS | Metrics & More | Article Recommendations | Supporting Information

ABSTRACT: In pathogens, a unique class of metalloregulator proteins, called gene regulatory proteins, sense specific metal ions that initiate gene transcription of proteins that export metal ions from the cell, thereby preventing toxicity and cell death. CsoR is a metalloregulator protein found in various bacterial systems that "sense" Cu(I) ions with high affinity. Upon copper binding, CsoR dissociates from the DNA promoter region, resulting in initiation of gene transcription. Crystal structures of CsoR in the presence and absence of Cu(I) from various bacterial systems have been reported, suggesting either a dimeric or tetrameric structure of these helical proteins. However, structural information about the CsoR-DNA complex is missing. Here, we applied electron paramagnetic resonance (EPR) spectroscopy to follow the conformational and dynamical changes that *Mycobacterium tuberculosis* CsoR undergoes upon DNA binding in solution. We showed that the quaternary structure is predominantly dimeric in solution, and only minor conformational and dynamical changes occur in the DNA bound state. Also, labeling of the unresolved C- terminus revealed no significant change in dynamics upon DNA binding. These observations are unique, since for other bacterial copper metalloregulators, such as the MerR and CopY families, major conformational changes were observed upon DNA binding, indicating a different mode of action for this protein family.

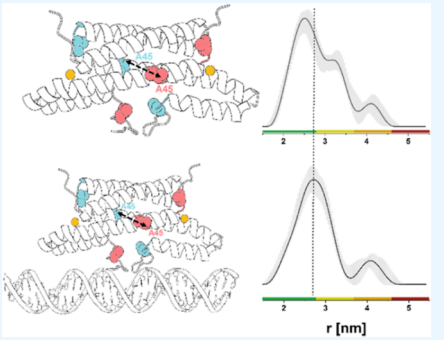

INTRODUCTION

Copper, along with other metals such as zinc and iron, are commonly found as natural prosthetic groups of proteins. However, copper ions are toxic when free in biological fluids, owing to their ability to cycle between two oxidation states, Cu(II) and Cu(I). This cycle between oxidation states results in reactive oxygen species (ROS) and ultimately leads to cell death. Hence, various microorganisms have evolved a highly sophisticated mechanism for copper homeostasis. They dedicated an entire regulatory machinery to acquire, utilize, traffic, detoxify, and otherwise manage the intracellular and extracellular concentrations of copper ions encountered in their microenvironment.[1−6] For pathogenic bacteria, the challenges are even harsher. These organisms face an ever-changing landscape of metal deprivation and toxicity in human hosts. Metal sensor proteins are unique metal-sensing transcription regulators found only in bacteria; they act as metal coordination sites that "sense" specific metal ions. To illustrate, *Mycobacterium tuberculosis*, a human pathogen responsible for at least 2 million deaths every year, encodes over 15 metal sensor proteins. When the metalloregulator protein (metal transcription factor) chelates a specific metal ion, it induces conformational changes in the protein's structure and dynamics that control the transcription mechanism. These conformational changes facilitate or prevent binding of the DNA promoter sequence and regulate transcription initiation. Thus, they control the transcription of genes, which encode proteins involved in metal homeostasis, including transporting proteins that import essential metals or export them if they are present in excess.[7−9]

The copper-sensing operon repressor (CsoR) is a member of a major Cu(I) sensing family of bacterial metalloregulator proteins that has evolved to prevent copper toxicity in the cytoplasm.[10−14] CsoR was first discovered in *M. tuberculosis*; other CsoRs were studied from *Bacillus subtilis*, *Staphylococcus aureus*, *Thermus thermophilus*, *Listeria monocytogenes*, and *Streptomyces lividness*.[15−20] The first crystal structure of CsoR from *M. tuberculosis* was reported in 2007; however, the last 30 amino acid residues of the C-terminus were not resolved.[14] CsoR (PDB-ID: 2HH7) crystallized as a homodimer.[21] Analysis of the protein interfaces with the Evolutionary Protein−protein Interface Classifier (EPPIC) showed that only one dimer interface is of biological nature, whereas the remaining interaction sites are crystallographic and experimental artifacts.[22] Interestingly, one of these crystallographic interfaces coincides with the predicted DNA binding site.[21,23] Thus, the crystal structure of CsoR (2HH7) only provides limited information about the DNA binding mechanism due to the crystallographic artifact and the lacking C-terminus.

Received: August 25, 2023
Accepted: September 28, 2023
Published: October 13, 2023

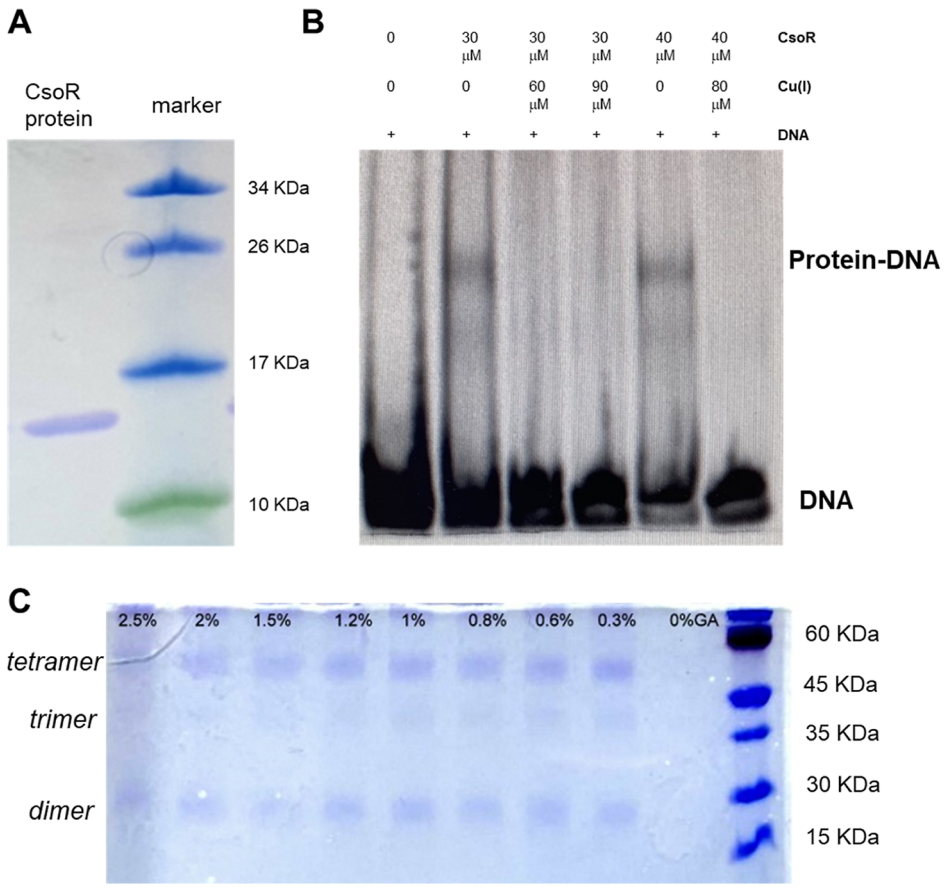

Figure 1. (A) SDS-PAGE gel of purified *M. tuberculosis* CsoR (13 kDa) was stained with coomassie brilliant blue. (B) EMSA gel of CsoR bound to a GC-rich DNA sequence as a function of different CsoR and Cu(I) concentration. (C) Cross-linking experiments were performed as a function of various concentrations of the glutaraldehyde (GA) cross-linker.

Nevertheless, this structure revealed that CsoR is an all α-helical protein with a four-helix bundle architecture (α1-α2-α1′-α2′) flanked by C-terminal α3/α3′ helices. CsoR binds one Cu(I) per monomer in an interdimer trigonal S_2N coordination via three residues: (1) Cys36 (α2 helix), (2) Cys65′ (α2′ helix) from the opposite monomer within the dimer, and (3) His61′ (α2′ helix). In the apo form (in the absence of Cu(I)), *M. tuberculosis* CsoR represses the transcription of the *cso* operon gene by binding to the gene's sequence (5′-GTAGCCCACCCCCAGTGGGGTGGGA-TAC-3′). In the holo-form (bound to Cu(I)), CsoR dissociates from the DNA, and transcription occurs. The *cso* operon encodes CsoR, in addition to a Cu(I)-efflux P-type ATPase, CtpV. The CsoR structure suggests that two CsoR dimers fold into a D_2-symmetric tetramer, and that two CsoR tetramers bind to one *cso* operon.[11] To date, no high-resolution structure of a DNA-bound CsoR complex has been reported. As a result, there is a general lack of molecular information that might provide insights into the regulation of the transcription mechanism.

EPR spectroscopy has emerged as an excellent tool for resolving such systems since it does not require crystallization and does not depend on protein size. EPR can be measured in buffer solution, and even a weak interaction between protein and DNA can be detected.[24−26] EPR's strength lies in its sensitivity to both changes on an atomic level and nanoscale fluctuations.[27−31] In addition, EPR can measure distances between paramagnetic probes within the protein, and between proteins, up to 10.0 nm.[32−43] Sometimes the measurement of one distance (or a few) is sufficient to establish the plausibility of a mechanism or to validate a proposed structure. The most common means for obtaining nanoscale structural information is by pulsed electron double resonance (PELDOR), also commonly termed the double electron resonance experiment (DEER). Pulsed EPR experiments can measure nanometer distances between paramagnetic probes, and continuous wave (CW) EPR can derive the dynamics of protein chains. The combination of CW and pulsed EPR with site-directed spin labeling (SDSL) has become widely used in biophysical research,[44−52] where an electron spin introduced into diamagnetic proteins provides information on their local environment and on the mobility of the protein domain. Herein, we applied SDSL, together with EPR spectroscopy, to target conformational changes in the CsoR protein upon DNA binding.

RESULTS

The gene encoding *M. tuberculosis* CsoR (119 amino acids) was cloned, expressed, and purified from *E. coli*. Figure 1A shows the SDS-PAGE gel of the purified CsoR protein. Figure 1B presents an electrophoresis mobility shift assay by a fluorescence (EMSA) gel picture of CsoR, confirming that CsoR binds the DNA only in the apo form, in the absence of Cu(I). To better understand the assembly of the protein, which will be required for the EPR data analysis, cross-linking experiments of CsoR as a function of different ratios of

https://doi.org/10.1021/acsomega.3c06336
ACS Omega 2023, 8, 39886−39895

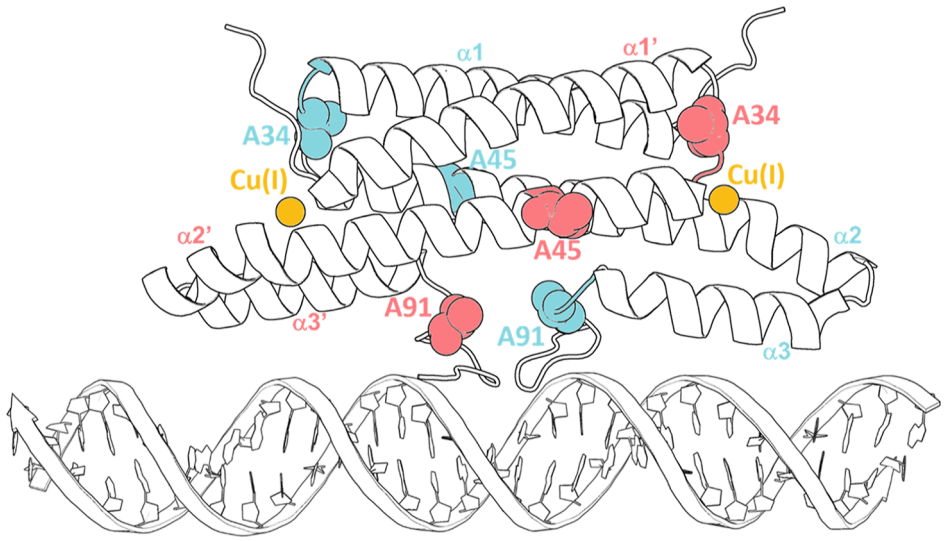

Figure 2. CsoR dimer model with proposed DNA binding site (PDB: 2HH7). The spin-labeling sites are marked in pink and cyan according to each monomer. Cu(I) sites are indicated with yellow spheres.

glutaraldehyde (the cross-linker) were performed (Figure 1C). It shows that this protein is either in a dimeric (26 kDa) or tetrameric (52 kDa) state. A weak trimer band was also observed at 39 kDa. We then used ConSurf[53] (Figure S1, Supporting Information) to pinpoint potential nonconserved residues that can be mutated to cysteine for SDSL with the 1-oxyl-2,2,5,5-tetramethylpyrroline-3-methylmethanethiosulfonate (MTSSL) nitroxide spin label (Figure S2, Supporting Information). The following point mutations were chosen: A34C mutation within the loop between α1 and α2 of the protein, the A45C mutation located on helix α2, and A91C on helix α3 (Figure 2). However, since we observed minor spin-labeling of about 10−20% of cysteine C36 and C65 that are involved in Cu(I) binding, we mutated these cysteine residues to methionine. The following mutations were prepared: CsoR_A34C_C36M_C65 M (termed CsoR_A34C), CsoR_A45C_C36M_C65 M (termed CsoR_A45C), and CsoR_A91C_C36M_C65 M (termed CsoR_A91C). Mass spectra and CW-EPR confirmed that the yield of the spin-labeling is above 90% (Figures S3 and S4, Supporting Information).CD spectra verified that these mutations do not interfere with the secondary structure of the protein (Figure S5, Supporting Information), and EMSA experiments confirmed that these mutants can bind to the DNA (Figure S6, Supporting Information).

DEER experiments were first performed for all of the mutants in the apo-state. Figure 3 presents the DEER time domain data and corresponding distance distribution functions. The DEER data suggest various conformations of the protein, which is characterized by broad distance distribution functions. Moreover, the predicted distance distribution, which corresponds to the CsoR crystal structure conformation (derived using the chiLife program[54] and PDB: 2HH7) as a dimer (orange line) and tetramer (green line) is presented, for all mutants in Figure 3. The DEER data proposed that the structure of CsoR in solution agrees well with the crystal structure. Moreover, the modulation depth for all DEER traces was in the same range of about 15−17%, which indicates that the assembly of CsoR is similar for all solutions. Based on the comparison with the predicted distance distributions of the crystal structure, it seems that the protein can exist both in dimeric and in tetrameric states. However, it seems that the contribution of the dimer to the distance distribution function is higher than the distances corresponding to the tetrameric assembly. SEC-HPLC data (Figure S7) confirmed that the protein exists in dimeric and tetrameric forms.

We then carried out DEER measurements on all mutants in the presence of DNA (Figures 4−6). No change in the distance distribution was observed for the CsoR_A34C mutant. For CsoR_A45C, a small shift in the mean distance from 2.5 nm in the absence of DNA, to 2.7 nm in the presence of DNA, in addition, a slight narrowing in the distribution upon DNA binding was detected. For CsoR_A91C, a slight shift in the mean distance from 2.1 to 2.2 nm upon DNA binding was also observed. The DEER data suggest minor opening between helices α2 and α3 upon DNA binding.

CW-EPR experiments were performed at room temperature (RT) on all spin-labeled proteins in the absence and presence of DNA (Figure 7). Differences in the mobility of the spin-labels at different sites were observed, where the lowest mobility was detected for A91C site (α3 helix). However, no significant change in dynamics for all sites was detected as a function of DNA binding. The CW-EPR spectra were analyzed using the easyspin program[56] (Figure S8, Table S1, Supporting Information). Some minor decreases in dynamics were detected for CsoR_A34C and CsoR_A45C upon DNA binding.

DISCUSSION

Bacteria rely on a unique and exclusive set of proteins to quickly adapt to metal ion toxicity or deprivation. These unique proteins are transcription factors that contain at least two domains: a metal coordination site, which "senses" specific metal ions, and a DNA-binding site. Both domains are responsible for inducing conformational changes in the protein and the DNA that eventually will lead to transcription.[57−60] Bacteria contain various metal-sensitive transcription factors that mediate metal homeostasis by regulating the expression of genes encoding metal transporters, intracellular chelators and/or other detoxification enzymes.[9,58,61] At present, seven major families of metal-sensitive transcription factors have been identified in bacteria (i.e., the ArsR, MerR, CsoR, CopY, Fur,

https://doi.org/10.1021/acsomega.3c06336
ACS Omega 2023, 8, 39886−39895

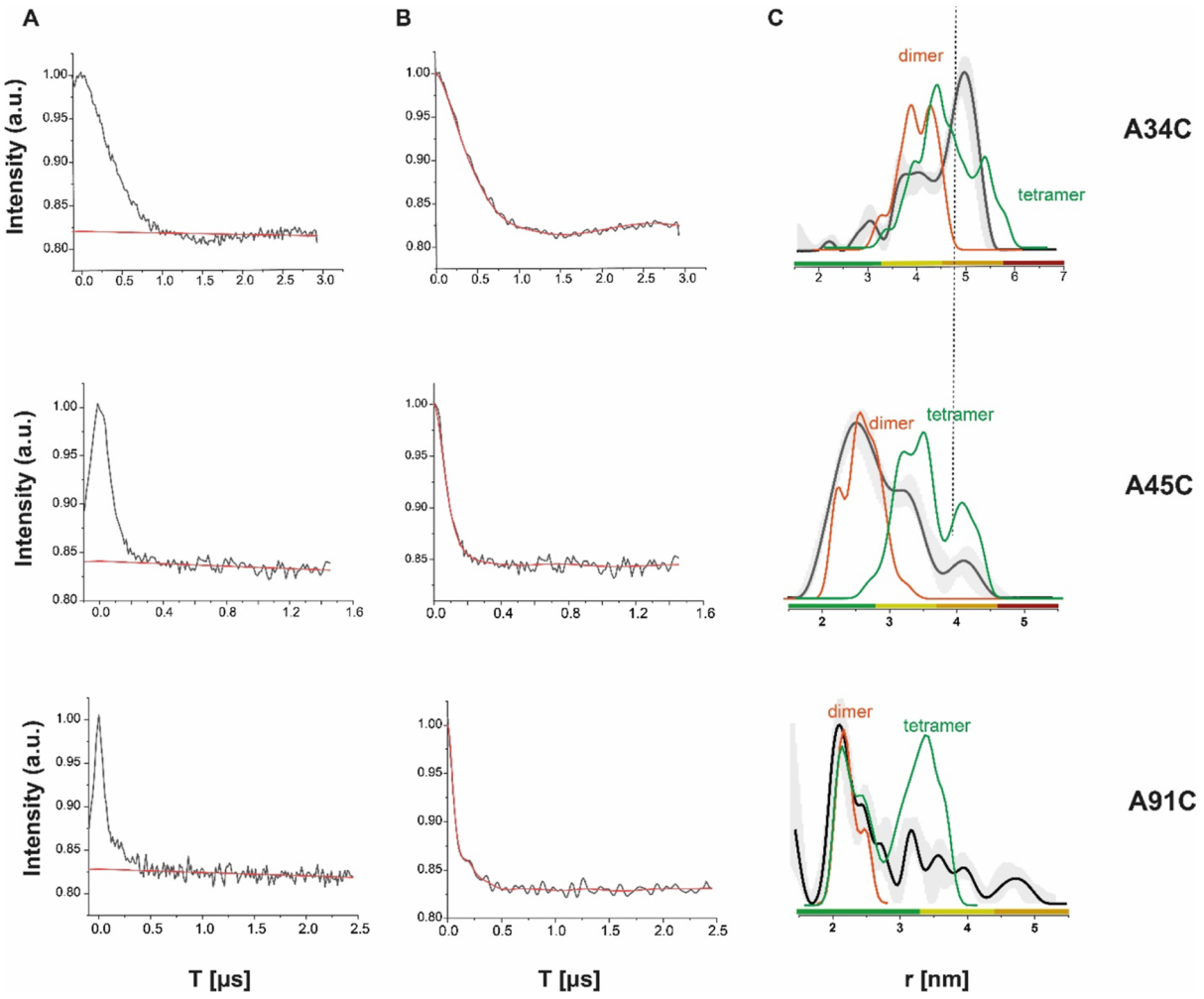

Figure 3. DEER data for the various CsoR mutants. (A) DEER time domain raw data (black); the red line represents the background function. (B) DEER time domain data after background subtraction (black) and the corresponding fit (red) obtained using DeerAnalysis program.[55] (C) Corresponding distance distribution function using Tikhonov regularization, where the regularization parameter was 30. The orange distance distributions and the green distance distributions represent the distance distribution function predicted using the chiLife program for the selected mutant based on the PDB: 2HH7 structure for the dimer and tetramer assembly. Distance distribution validation considered white noise, background start, and dimensionality. The color bar indicates the reliability of the distance distributions (green: shape reliable; yellow: mean and width reliable; orange: mean reliable; red: no quantification possible). Purified protein concentration was between 60 and 80 μM. For all samples 30% glycerol was added.

Dtx1, and NikR families), with at least one crystal structure of at least one representative of these seven families has been reported.[8,9,58,61] Proteins from the same family share sequence similarities of 30−60%, and thus greatly resemble each other. X-ray crystallography, NMR, and Cryo-EM techniques have been able to report on different structures of these proteins, especially when they are bound to the specific metal ion. However, targeting different conformations as a function of metal ion concentration and DNA, which provides a better understanding of the mechanism of action of these proteins, is more challenging.[7,62−65] EPR spectroscopy can overcome these gaps since it can follow conformational and dynamical changes in solution and in-cell upon DNA and metal ion binding.[66−68] In our lab, we have been implementing EPR measurements on *E. coli* CueR, *S. pneumoniae* CopY, and the current study on *M. tuberculosis* CsoR. Figure 8 summarizes the structural changes observed for the three transcription factors using EPR measurements. For *M. tuberculosis* CsoR (Figure 8A), minor changes, where helices α2 and α3 are spreading apart by 1−2 Å, were detected upon DNA binding. For *E. coli* CueR (Figure 8B), major structural changes were observed, where the two α2 helices in the DNA binding domain are spreading apart by about 10 Å, while the two α4 helices are getting closer to each other by about 8 Å.[24,25,69] The DNA binding domain that involves helices α1-α4 exhibits additional conformational changes upon metal ion binding. However, no changes in kinetics were detected for *E. coli* CueR as a function of DNA binding, only as a function of metal ion coordination.[70] For *S. pneumoniae* CopY (Figure 8C), major dynamical and conformational changes were detected upon DNA binding, where the dynamics in the dimer interface and the metal binding site becomes completely restricted upon DNA binding, and the two-dimer interface regions of CopY are spreading apart by 13 Å, while the two metal binding sites are getting closer to each other by 5 Å.[71] As compared to CueR and CopY, the CsoR mechanism appears to be entirely different upon DNA binding. This suggests a unique feature of this repressor as compared to other copper transcription factors.[23] It was previously reported that mutagenesis of all three residues Arg15 and Arg52 and Cys36 abolished DNA

https://doi.org/10.1021/acsomega.3c06336
ACS Omega 2023, 8, 39886−39895

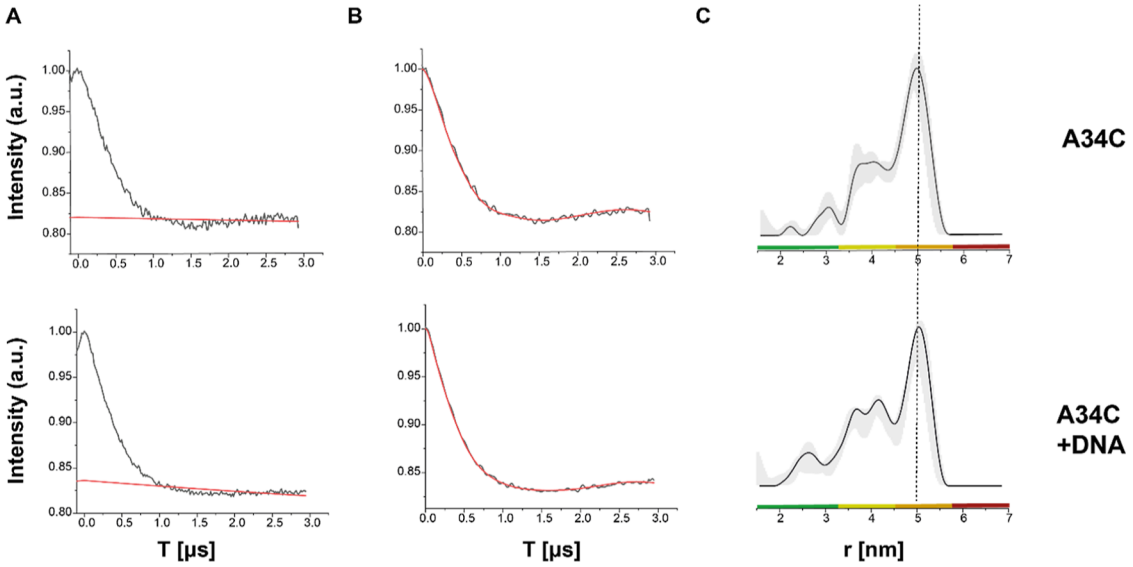

Figure 4. DEER data for the CsoR_A34C mutant in the presence and absence of DNA. (A) DEER time domain raw data (black), the red line represents the background function. (B) DEER time domain data after background subtraction (black) and the corresponding fit (red) obtained using DeerAnalysis program and Tikhonov regularization.[55] (C) Corresponding distance distribution function. Distance distribution validation considered white noise, background start, and dimensionality. The color bar indicates reliability of the distance distributions (green: shape reliable; yellow: mean and width reliable; orange: mean reliable; red: no quantification possible).

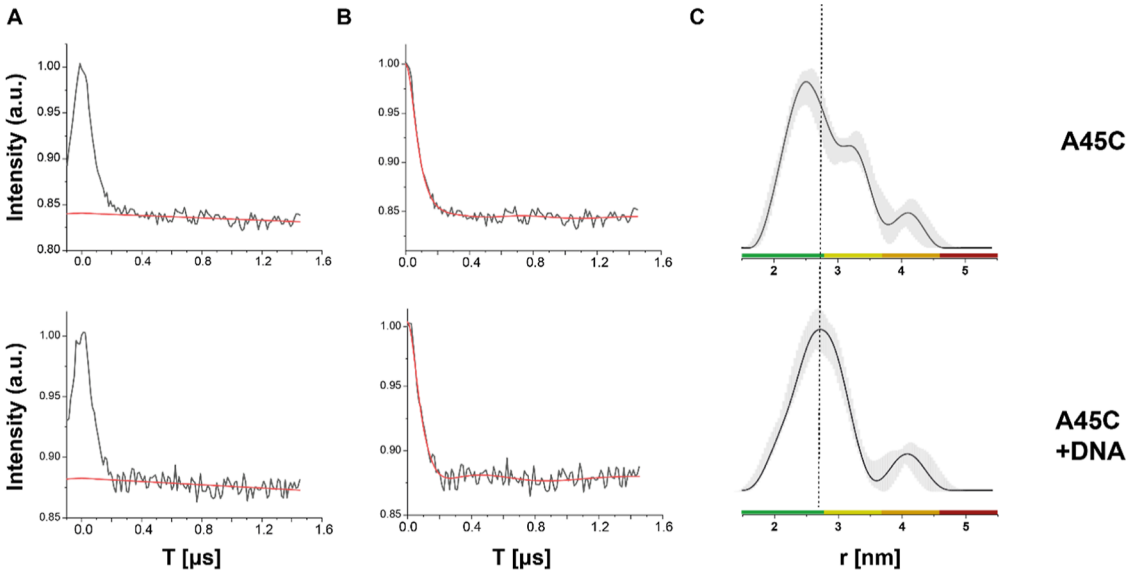

Figure 5. DEER data for the CsoR_A45C mutant in the presence and absence of DNA. (A) DEER time domain raw data (black), the red line represents the background function. (B) DEER time domain data after background subtraction (black) and the corresponding fit (red) obtained using DeerAnalysis program and Tikhonov regularization.[55] (C) Corresponding distance distribution function. Distance distribution validation considered white noise, background start, and dimensionality. The color bar indicates reliability of the distance distributions (green: shape reliable; yellow: mean and width reliable; orange: mean reliable; red: no quantification possible).

binding.[21] There, they proposed a crucial interaction between the copper binding site and C-terminal Glu81, allowing CsoR to dissociate from the DNA upon copper binding. Our study revealed no significant conformational changes upon DNA binding. Therefore, further studies are required to understand the complex interplay between metal ions and DNA binding on dynamical and conformational changes of CsoR. Moreover, DNA labeling will be applied to fully understand the conformational changes that occur within the promoter region during binding and dissociation of CsoR. Altogether, only comprehensive data including all factors will allow for a detailed understanding of the enigmatic transcription regulation by CsoR.

CONCLUSIONS

CsoR is a copper-sensitive repressor found in many bacterial systems. The reported structure of CsoR was resolved in various bacterial systems; however, it is available only in the absence of DNA. The structure suggests an alpha helical structure in a dimer or tetramer assembly. Here, we performed EPR measurements on CsoR as a function of DNA binding in solution. We showed that also in solution CsoR can exist in

https://doi.org/10.1021/acsomega.3c06336
ACS Omega 2023, 8, 39886−39895

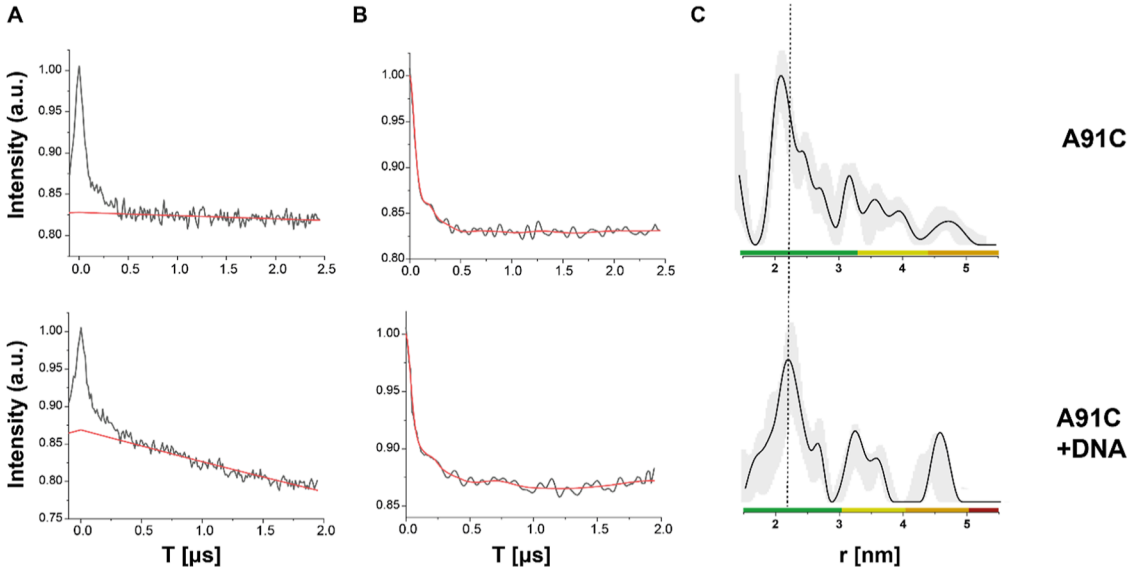

Figure 6. DEER data for the CsoR_A91C mutant in the presence and absence of DNA. (A) DEER time domain raw data (black), the red line represents the background function. (B) DEER time domain data after background subtraction (black) and the corresponding fit (red) obtained using DeerAnalysis program and Tikhonov regularization.[55] (C) Corresponding distance distribution function. Distance distribution validation considered white noise, background start, and dimensionality. The color bar indicates reliability of the distance distributions (green: shape reliable; yellow: mean and width reliable; orange: mean reliable; red: no quantification possible).

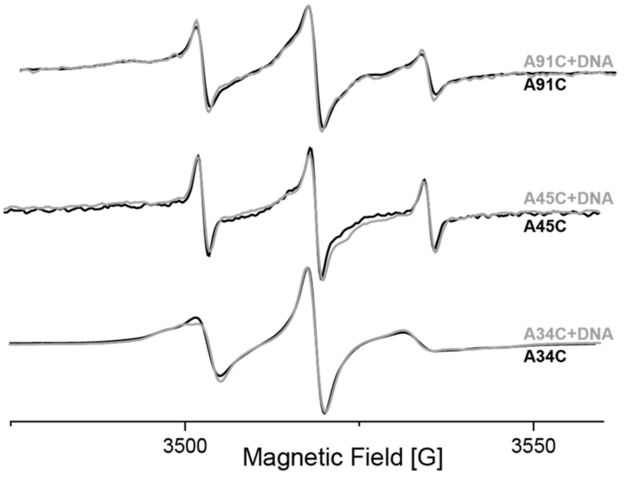

Figure 7. RT CW-EPR experiments in the absence (black lines) and presence (gray lines) of DNA, for the different mutants.

both dimeric and tetrameric states. Interestingly, only minor dynamical and conformational changes were determined as a function of DNA binding including the unresolved C-terminus. This behavior is unique to this transcription factor because other bacterial copper transcription factors showed major conformational and dynamical changes upon DNA binding, which explain the mechanism of action. It reveals our lack of understanding of gene transcription regulation by CsoR. Hence, further research is required to shed light on this enigmatic process triggered by copper binding.

MATERIALS AND METHODS

Cloning, Expression, and Purification of CsoR. CsoR was cloned in modified pET28a by PCR, and the resulting plasmid was confirmed by DNA sequencing. The plasmid was transformed into *E. coli* BL21 and grown in LB media at 37 °C until the OD_{600} reached 0.5. Then 1 mM isopropyl-β-D-thiogalactopyranoside (IPTG, Bio-Lab) was added. After an additional overnight incubation at 18 °C, cells were separated by centrifugation. Bacterial pellets were resuspended in buffer containing 25 mM Tris-HCl (Bio-Lab) pH 7.4, 250 mM NaCl (Fisher Bioreagents),10 mM imidazole (Fisher Bioreagents), treated with homogenizer, and then passed through a Microfluidizer processor. Next, 2 mM PMSF protease inhibitor (Sigma-Aldrich) was added to the lysed culture and centrifuged at 14,000 rpm and 4 °C for 40 min. The protein lysate in the soluble fraction was purified with Ni-NTA beads (Cytiva) according to the manufacturer's instructions.

CsoR Spin-Labeling. The protein was spin-labeled with *S*-(2,2,5,5-tetramethyl-2,5-dihydro-1*H*-pyrrol-3-yl) methylmethane-thiosulfonothiate (MTSSL, TRC). CsoR elution fractions were incubated with 10 mM DTT (Holland Moran) to reduce potential disulfide bonds and dialyzed against Tris buffer [25 mM Tris (pH 7.4), 250 mM NaCl], using 1 kDa dialysis cassettes, at 4 °C for 12 h, to remove free DTT. The protein was subsequently incubated with 15 mM MTSSL, vortexed overnight at 4 °C, and dialyzed against Tris buffer at 4 °C for 72 h, to remove free MTSSL.

Mass-Spec Analysis. Liquid chromatography mass spectrometry (LC−MS) analysis was performed on a 6545 QTOF mass spectrometer (Agilent) that was equipped with an electrospray ionization (ESI) coupled to a 1260 UHPLC. UHPLC was carried out on a Agilent Infinity Lab Poroshell 120 EC-C1850 × 4.6 mm, 2.7 μm column.

Circular Dichroism Experiments. Circular dichroism (CD) measurements were conducted by using a Chirascan spectrometer. Measurements were carried out over a range of 20−90 °C in a 1 mm optical path length cell, and the spectra were recorded from 190 to 260 nm. The CD signal was an average of 3 scans for each sample.

HPLC-SEC Experiments. HPLC measurements were performed using a PSS PROTEEMA 5 μ column with dimensions 300 mm × 8.0 mm on an Agilent 1260 Infinity II LC System. The column was calibrated using protein

https://doi.org/10.1021/acsomega.3c06336
ACS Omega 2023, 8, 39886−39895

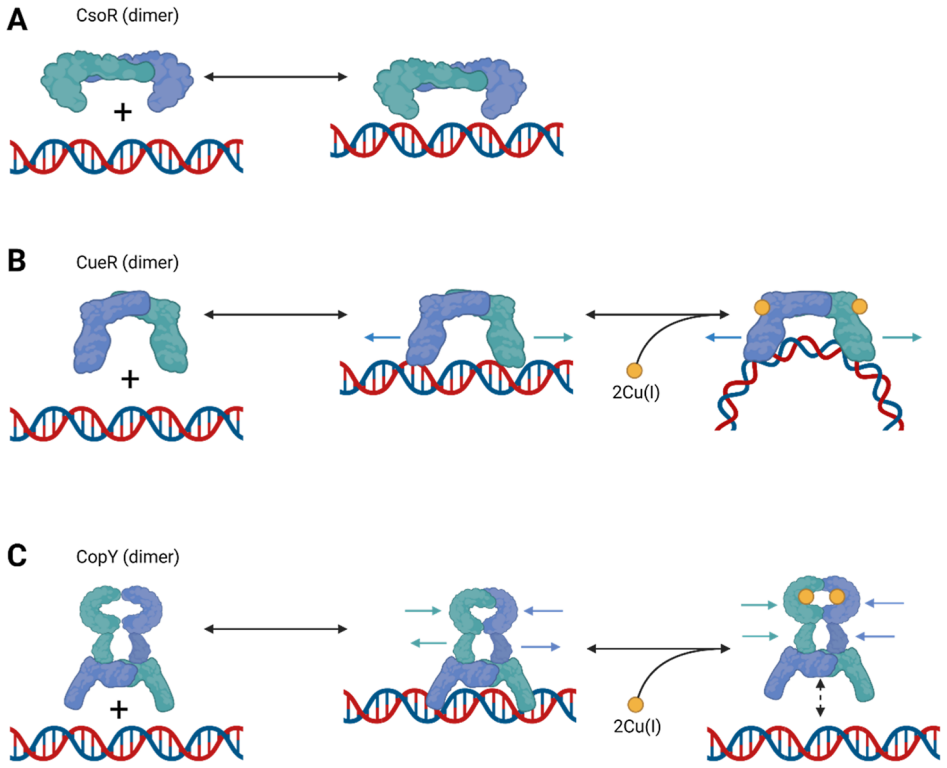

Figure 8. Schematic illustration for the mechanism of action of the following copper transcription factors: (A) *M. tuberculosis* CsoR. (B) *E. coli* CueR and (C) *S. pneumoniae* CopY based on EPR measurements. The arrows mark the direction of movement of the protein's domains.

standard mix 15−600 kDA (Thyroglobulin bovine 670 kDa, gamma-globulins 150 kDa, ovalbumin 44.3 kDa, ribonuclease A 13.7 kDa, *p*-aminobenzoic acid 137 Da) (Sigma-Aldrich) using buffer containing 25 mM Tris-base (Fisher Bioreagents) pH 7.4, 250 mM NaCl, 10 mM imidazole with an isocratic flow rate of 0.75 mL/min for 25 min and absorbance detection of UV-280 nm.

Cross-Linking Experiments. Cross-linking reactions were carried out with different ratios of glutaraldehyde (GA, Sigma-Aldrich) and CsoR protein at RT for 30 min in buffer containing 25 mM Hepes (Biological Industries) and 250 mM NaCl in a 40 μL final volume. The reactions were stopped by Tris-HCl buffer pH = 7.4 in a final concentration of 125 mM. Regarding the cross-linking experiments with copper, the proteins were incubated for 30 min with Cu(I) (Sigma-Aldrich) at different ratios and then for 30 min with GA at RT.

Electrophoretic Mobility Shift Assay Experiment. The GC-rich DNA sequence that binds CsoR protein was labeled using cy5 fluorescent dye. A protein−DNA complex was formed in 40 μL of incubation buffer [25 mM Tris-base pH 7.4, 250 mM NaCl, 5% vol/vol glycerol (Sigma-Aldrich)] for 30 min at RT, and then formaldehyde cross-linking assays were performed. Formaldehyde (Fisher Bioreagents) was added to a final concentration of 0.74%, and the reactions were incubated for an additional 30 min on ice. The cross-linked protein−DNA complexes were resolved on 4.5% (37:1) native polyacrylamide gels that were prerun at 20 mA for 1 h. The samples were loaded onto the gel running at 10 mA for an additional hour. The gels were imaged by a typhoon phosphorimager (Typhoon FLA9500).

Addition of DNA. For EPR measurements, the duplex sequence of (GC-rich) DNA (Integrated DNA Technologies) was added to apo-CsoR and holo-CsoR in ratio 2:1 protein: DNA (5′-GTAGCCCACCCCCAGTGGGGTGGGATAC-3′).

X-Band CW-EPR Experiments. CW-EPR spectra were recorded using an E500 Elexsys Bruker spectrometer operating at 9.0−9.5 GHz and equipped with a superhigh-sensitivity CW resonator. The spectra were recorded at room temperature (292 ± 5 K), at a microwave power of 20.0 mW, a modulation amplitude of 1.0 G, a time constant of 60 ms, and a receiver gain of 60.0 dB. The samples were measured in 1.0 mm quartz tubes (Wilmad-LabGlass, Vineland, NJ). CW-EPR simulations were carried out using MATLAB, with the EasySpin toolbox.[56]

Q-Band DEER Experiments. The DEER experiment $\pi/2(\nu_{obs}) - \tau_1 - \pi(\nu_{obs}) - T - \pi(\nu_{pump}) - (\tau_1 + \tau_2 - T) - \pi(\nu_{obs}) - \tau_2 -$ echo was carried out at 50 ± 1.0 K on a Q-band Elexsys E580 spectrometer, equipped with a 2 mm resonator and a 50 W traveling wave tube amplifier. A two-step phase cycle was employed on the first pulse. The echo was measured as a function of T, and τ_2 was kept constant to eliminate any relaxation effects. The durations of the observer and the pump π pulse were 24 ns each. The dwell time was 12 ns. τ_1 was set to 200 ns, and τ_2 was set to 1400−3200 ns. The pump pulse was set to the maximum of the nitroxide spectrum, and the observer was set 70 MHz higher. The samples were measured in 1.6 mm capillary quartz tubes (Wilmad-LabGlass). The data were analyzed using the DeerAnalysis program.[55,72]

■ ASSOCIATED CONTENT

Supporting Information

The Supporting Information is available free of charge at https://pubs.acs.org/doi/10.1021/acsomega.3c06336.

Sequence conservation analysis of CsoR by ConSurf, reaction scheme of cysteine residue spin labeling with MTSSL, mass spectrometry data of spin-labeled CsoR,

https://doi.org/10.1021/acsomega.3c06336
ACS Omega 2023, 8, 39886−39895

spin-labeling efficiency, CD spectra of CsoR and mutants, EMSA gel of CsoR and mutants, HPLC-SEC results of CsoR and mutants, CW-EPR spectra and simulations (PDF)

Accession Codes

Accession Uniport ID no. of CsoR protein: P9WP49. NCBI Accession: ANZ81610.1.

AUTHOR INFORMATION

Corresponding Author

Sharon Ruthstein − *Department of Chemistry and the Institute of Nanotechnology and Advanced Materials (BINA), Bar-Ilan University, Ramat-Gan 52900, Israel;* orcid.org/0000-0002-1741-6892; Phone: +972-3-7384329; Email: Sharon.ruthstein@biu.ac.il

Authors

Yasmin Igbaria-Jaber − *Department of Chemistry and the Institute of Nanotechnology and Advanced Materials (BINA), Bar-Ilan University, Ramat-Gan 52900, Israel*

Lukas Hofmann − *Department of Chemistry and the Institute of Nanotechnology and Advanced Materials (BINA), Bar-Ilan University, Ramat-Gan 52900, Israel*

Lada Gevorkyan-Airapetov − *Department of Chemistry and the Institute of Nanotechnology and Advanced Materials (BINA), Bar-Ilan University, Ramat-Gan 52900, Israel*

Yulia Shenberger − *Department of Chemistry and the Institute of Nanotechnology and Advanced Materials (BINA), Bar-Ilan University, Ramat-Gan 52900, Israel*

Complete contact information is available at: https://pubs.acs.org/10.1021/acsomega.3c06336

Notes

The authors declare no competing financial interest.

ACKNOWLEDGMENTS

S.R. acknowledges the support of the Israel Science Foundation (grant no. 176/16).

REFERENCES

(1) Hofmann, L.; Hirsch, M.; Ruthstein, S. Advances in Understanding of the Copper Homeostasis in Pseudomonas aeruginosa. *Int. J. Mol. Sci.* **2021**, *22*, 2050.

(2) Bertinato, J.; L'Abbe, M. R. Maintaining copper homeostasis: regulation of copper-trafficking proteins in response to copper deficiency or overload. *J. Nutr. Biochem.* **2004**, *15*, 316−322.

(3) Burkhead, J. L.; Gogolin Reynolds, K. A.; Abdel-Ghany, S. E.; Cohu, C. M.; Pilon, M. Copper Homeostasis. *New Phytol.* **2009**, *182*, 799−816.

(4) Gaggelli, E.; Kozlowski, H.; Valensin, D.; Valensin, G. Copper Homeostasis and Neurodegenerative Disorders (Alzheimer's, Prion, and Parkinson's Diseases and Amyotrophic Lateral Sclerosis). *Chem. Rev.* **2006**, *106*, 1995−2044.

(5) Li, C.; Li, Y.; Ding, C. The Role of Copper Homeostasis at the Host-Pathogen Axis: From Bacteria to Fungi. *Int. J. Mol. Sci.* **2019**, *20*, 175.

(6) Lutsenko, S. Human copper homeostasis: a network of interconnected pathways. *Curr. Opin. Chem. Biol.* **2010**, *14*, 211−217.

(7) Changela, A.; Chen, K.; Xue, Y.; Holschen, J.; Outten, C. E.; O'Halloran, T. V.; Mondragón, A. Molecular basis of metal-ion selectivity and zeptomolar sensitivity by CueR. *Science* **2003**, *301*, 1383−1387.

(8) Waldron, K. J.; Rutherford, J. C.; Ford, D.; Robinson, N. J. Metalloproteins and metal sensing. *Nature* **2009**, *460*, 823−830.

(9) Tottey, S.; Harvie, D. R.; Robinson, N. J. Understanding How Cells Allocate Metals Using Metal Sensors and Metallochaperones. *Acc. Chem. Res.* **2005**, *38*, 775−783.

(10) Jacobs, A. D.; Chang, F. M. J.; Morrison, L.; Dilger, J. M.; Wysocki, V. H.; Clemmer, D. E.; Giedroc, D. P. Resolution of Stepwise Cooperativities of Copper Binding by the Homotetrameric Copper-Sensitive Operon Repressor (CsoR): Impact on Structure and Stability. *Angew. Chem., Int. Ed.* **2015**, *54*, 12795−12799.

(11) Chang, F. M. J.; Martin, J. E.; Giedroc, D. P. Electrostatic Occlusion and Quaternary Structural Ion Pairing Are Key Determinants of Cu(I)-Mediated Allostery in the Copper-Sensing Operon Repressor (CsoR). *Biochemistry* **2015**, *54*, 2463−2472.

(12) Chang, F. M. J.; Coyne, H. J.; Cubillas, C.; Vinuesa, P.; Fang, X. Y.; Ma, Z.; Ma, D. J.; Helmann, J. D.; Garcia-de los Santos, A.; Wang, Y. X.; Dann, C. E.; Giedroc, D. P. Cu(I)-mediated Allosteric Switching in a Copper-sensing Operon Repressor (CsoR). *J. Biol. Chem.* **2014**, *289*, 19204−19217.

(13) Higgins, K. A.; Giedroc, D. Insights into Protein Allostery in the CsoR/RcnR Family of Transcriptional Repressors. *Chem. Lett.* **2014**, *43*, 20−25.

(14) Liu, T.; Ramesh, A.; Ma, Z.; Ward, S. K.; Zhang, L. M.; George, G. N.; Talaat, A. M.; Sacchettini, J. C.; Giedroc, D. P. CsoR is a novel Mycobacterium tuberculosis copper-sensing transcriptional regulator. *Nat. Chem. Biol.* **2007**, *3*, 60−68.

(15) Smaldone, G. T.; Helmann, J. D. CsoR regulates the copper efflux operon copZA in Bacillus subtilis. *Microbiology* **2007**, *153*, 4123−4128.

(16) Ma, Z.; Cowart, D. M.; Scott, R. A.; Giedroc, D. P. Molecular insights into the metal selectivity of the copper(I)-sensing repressor CsoR from Bacillus subtilis. *Biochemistry* **2009**, *48*, 3325−3334.

(17) Baker, J.; Sengupta, M.; Jayaswal, R. K.; Morrissey, J. A. The Staphylococcus aureus CsoR regulates both chromosomal and plasmid-encoded copper resistance mechanisms. *Environ. Microbiol.* **2011**, *13*, 2495−2507.

(18) Sakamoto, K.; Agari, Y.; Agari, K.; Kuramitsu, S.; Shinkai, A. Structural and functional characterization of the transcriptional repressor CsoR from Thermus thermophilus HB8. *Microbiology* **2010**, *156*, 1993−2005.

(19) Corbett, D.; Schuler, S.; Glenn, S.; Andrew, P. W.; Cavet, J. S.; Roberts, I. S. The combined actions of the copper-responsive repressor CsoR and copper-metallochaperone CopZ modulate CopA-mediated copper efflux in the intracellular pathogen Listeria monocytogenes. *Mol. Microbiol.* **2011**, *81*, 457−472.

(20) Dwarakanath, S.; Chaplin, A. K.; Hough, M. A.; Rigali, S.; Vijgenboom, E.; Worrall, J. A. R. Response to copper stress in Streptomyces lividans extends beyond genes under direct control of a copper-sensitive operon repressor protein (CsoR). *J. Biol. Chem.* **2012**, *287*, 17833−17847.

(21) Liu, T.; Ramesh, A.; Ma, Z.; Ward, S. K.; Zhang, L.; George, G. N.; Talaat, A. M.; Sacchettini, J. C.; Giedroc, D. P. CsoR is a novel Mycobacterium tuberculosis copper-sensing transcriptional regulator. *Nat. Chem. Biol.* **2007**, *3*, 60−68.

(22) Bliven, S.; Lafita, A.; Parker, A.; Capitani, G.; Duarte, J. M. Automated evaluation of quaternary structures from protein crystals. *PLoS Comput. Biol.* **2018**, *14*, No. e1006104.

(23) Higgins, K. A.; Giedroc, D. Insights into Protein Allostery in the CsoR/RcnR Family of Transcriptional Repressors. *Chem. Lett.* **2014**, *43*, 20−25.

(24) Sameach, H.; Ghosh, S.; Gevorkyan-Airapetov, L.; Saxena, S.; Ruthstein, S. EPR Spectroscopy Detects Various Active State Conformations of the Transcriptional Regulator CueR. *Angew. Chem., Int. Ed.* **2019**, *58*, 3053−3056.

(25) Sameach, H.; Narunsky, A.; Azoulay-Ginsburg, S.; Gevorkyan-Aiapetov, L.; Zehavi, Y.; Moskovitz, Y.; Juven-Gershon, T.; Ben-Tal, N.; Ruthstein, S. Structural and Dynamics Characterization of the MerR Family Metalloregulator CueR in its Repression and Activation States. *Structure* **2017**, *25*, 988−996.e3.

(26) Sameach, H.; Ruthstein, S. EPR Distance Measurements as a Tool to Characterize Protein-DNA Interactions. *Isr. J. Chem.* **2019**, *59*, 980−989.
(27) Freed, J. H. *Multiple Electron Resonance Spectroscopy*; Plenum: New York, 1979.
(28) Hemminga, M. A.; Berliner, L. J. *ESR Spectroscopy in Membrane Biophysics*; Springer Science + Business Media, LLC: New York, 2007.
(29) Kevan, L. S. R. N. *Time Domain Electron Spin Resonance*; Wiley: New York, 1979.
(30) Schweiger, A.; Jeschke, G. *Principles of Electron Paramganetic Resonance*; University press: Oxford, 2001.
(31) Weil, J. A.; Bolton, J. R. *Electron Paramagnetic Resonance: Elementary Theory and Practical Applications*, 2nd ed.; John Wiley & Sons: New Jersey, 2007.
(32) Stratmann, L. M.; Kutin, Y.; Kasanmascheff, M.; Clever, G. H. Precise Distance Measurements in DNA G-Quadruplex Dimers and Sandwich Complexes by Pulsed Dipolar EPR Spectroscopy. *Angew. Chem., Int. Ed. Engl.* **2021**, *60*, 4939−4947.
(33) Widder, P.; Schuck, J.; Summerer, D.; Drescher, M. Combining site-directed spin labeling in vivo and in-cell EPR distance determination. *Phys. Chem. Chem. Phys.* **2020**, *22*, 4875−4879.
(34) Domnick, C.; Eggert, F.; Wuebben, C.; Bornewasser, L.; Hagelueken, G.; Schiemann, O.; Kath-Schorr, S. EPR Distance Measurements on Long Non-coding RNAs Empowered by Genetic Alphabet Expansion Transcription. *Angew. Chem., Int. Ed. Engl.* **2020**, *59*, 7891−7896.
(35) Heinz, M.; Erlenbach, N.; Stelzl, L. S.; Thierolf, G.; Kamble, N. R.; Sigurdsson, S. T.; Prisner, T. F.; Hummer, G. High-resolution EPR distance measurements on RNA and DNA with the non-covalent Ǵ spin label. *Nucleic Acids Res.* **2020**, *48*, 924−933.
(36) Jeschke, G. MMM: Integrative ensemble modeling and ensemble analysis. *Protein Sci.* **2021**, *30*, 125−135.
(37) Yang, Z.; Stein, R. A.; Ngendahimana, T.; Pink, M.; Rajca, S.; Jeschke, G.; Eaton, S. S.; Eaton, G. R.; McHaourab, H. S.; Rajca, A. Supramolecular Approach to Electron Paramagnetic Resonance Distance Measurement of Spin-Labeled Proteins. *J. Phys. Chem. B* **2020**, *124*, 3291−3299.
(38) Spicher, S.; Abdullin, D.; Grimme, S.; Schiemann, O. Modeling of spin-spin distance distributions for nitroxide labeled biomacromolecules. *Phys. Chem. Chem. Phys.* **2020**, *22*, 24282−24290.
(39) Yang, Y.; Pan, B. B.; Tan, X.; Yang, F.; Liu, Y.; Su, X. C.; Goldfarb, D. In-Cell Trityl-Trityl Distance Measurements on Proteins. *J. Phys. Chem. Lett.* **2020**, *11*, 1141−1147.
(40) Barth, K.; Rudolph, M.; Diederichs, T.; Prisner, T. F.; Tampe, R.; Joseph, B. Thermodynamic Basis for Conformational Coupling in an ATP-Binding Cassette Exporter. *J. Phys. Chem. Lett.* **2020**, *11*, 7946−7953.
(41) Sanaeifar, N.; Mader, K.; Hinderberger, D. Nanoscopic Characterization of Stearic Acid Release from Bovine Serum Albumin Hydrogels. *Macromol. Biosci.* **2020**, *20*, No. e2000126.
(42) Peter, M. F.; Bountra, K.; Beis, K.; Hagelueken, G. PELDOR/DEER: An Electron Paramagnetic Resonance Method to Study Membrane Proteins in Lipid Bilayers. *Methods Mol. Biol.* **2020**, *2168*, 313−333.
(43) Wort, J. L.; Ackermann, K.; Giannoulis, A.; Stewart, A. J.; Norman, D. G.; Bode, B. E. Sub-Micromolar Pulse Dipolar EPR Spectroscopy Reveals Increasing CuII-labelling of Double-Histidine Motifs with Lower Temperature. *Angew. Chem., Int. Ed.* **2019**, *58*, 11681−11685.
(44) Cai, Q.; Kusnetzow, A. K.; Hubbell, W. L.; Haworth, I. S.; Gacho, G. P. C.; Van Eps, N.; Hideg, K.; Chambers, E. J.; Qin, P. Z. Site-directed spin labeling measurements of nanometer distances in nucleic acids using a sequence-independent nitroxide probe. *Nucleic Acids Res.* **2006**, *34*, 4722−4730.
(45) Columbus, L.; Hubbell, W. L. A new spin on protein dynamics. *Trends Biochem. Sci.* **2002**, *27*, 288−295.
(46) Mchaourab, H. S.; Oh, K. J.; Fang, C. J.; Hubbell, W. L. Conformation of T4 Lysozyme in Solution. Hinge-Bending Motion and the Substrate-Induced Conformational Transition Studied by Site-Directed Spin Labeling. *Biochemistry* **1997**, *36*, 307−316.
(47) Shin, Y.-K.; Levinthal, C.; Levinthal, F.; Hubbell, W. L. Colicin E1 binding to membranes: Time-resolved studies of spin-labeled mutants. *Science* **1993**, *259*, 960−963.
(48) Vamvouka, M.; Cieslak, J.; Van Eps, N.; Hubbell, W.; Gross, A. The Structure of the Lipid-Embedded Potassium Channel Voltage Sensor Determined by Double-Electron-Electron Resonance Spectroscopy. *Protein Sci.* **2008**, *17*, 506−517.
(49) Zaccak, M.; Qasem, Z.; Gevorkyan-Airapetov, L.; Ruthstein, S. An EPR Study on the Interaction between the Cu(I) Metal Binding Domains of ATP7B and the Atox1Metallochaperone. *Int. J. Mol. Sci.* **2020**, *21*, 5536.
(50) Qasem, Z.; Pavlin, M.; Ritacco, I.; Gevorkyan-Airapetov, L.; Magistrato, A.; Ruthstein, S. The pivotal role of MBD4-ATP7B in the human Cu(i) excretion path as revealed by EPR experiments and all-atom simulations. *Metallomics* **2019**, *11*, 1288−1297.
(51) Levy, A. R.; Yarmiayev, V.; Moskovitz, Y.; Ruthstein, S. Probing the structural flexibility of the human copper metallochaperone Atox1 dimer and its interaction with the CTR1 c-terminal domain. *J. Phys. Chem. B* **2014**, *118*, 5832−5842.
(52) Meron, S.; Shenberger, Y.; Ruthstein, S. The Advantages of EPR Spectroscopy in Exploring Diamagnetic Metal Ion Binding and Transfer Mechanisms in Biological Systems. *Magnetochemistry* **2021**, *8*, 3.
(53) Armon, A.; Graur, D.; Ben-Tal, N. ConSurf: an algorithmic tool for the identification of functional regions in proteins by surface mapping of phylogenetic information. *J. Mol. Biol.* **2001**, *307*, 447−463.
(54) Tessmer, M. H.; Stoll, S. chiLife: An open-source Python package for in silico spin labeling and integrative protein modeling. *PLoS Comput. Biol.* **2023**, *19*, No. e1010834.
(55) Jeschke, G.; Chechik, V.; Ionita, P.; Godt, A.; Zimmermann, H.; Banham, J.; Timmel, C. R.; Hilger, D.; Jung, H. DeerAnalysis2006 - a Comprehensive Software Package for Analyzing Pulsed ELDOR Data. *Appl. Magn. Reson.* **2006**, *30*, 473−498.
(56) Stoll, S.; Schweiger, A. EasySpin, a comprehensive software package for spectral simulation and analysis in EPR. *J. Magn. Reson.* **2006**, *178*, 42−55.
(57) Foster, A. W.; Patterson, C. J.; Pernil, R.; Hess, C. R.; Robinson, N. J. Cytosolic Ni(II) sensor in cyanobacterium: nickel detection follows nickel affinity across four families of metal sensors. *J. Biol. Chem.* **2012**, *287*, 12142−12151.
(58) Giedroc, D. P.; Arunkumar, A. I. Metal sensor proteins: nature's metalloregulated allosteric switches. *Dalton Trans.* **2007**, *29*, 3107−3120.
(59) Novoa-Aponte, L.; Ramirez, D.; Arguello, J. M. The interplay of the metallosensor CueR with two distinct CopZ chaperones defines copper homeostasis in Pseudomonas aeruginosa. *J. Biol. Chem.* **2019**, *294*, 4934−4945.
(60) Osman, D.; Martini, M. A.; Foster, A. W.; Chen, J.; Scott, A. J. P.; Morton, R. J.; Steed, J. W.; Lurie-Luke, E.; Huggins, T. G.; Lawrence, A. D.; Deery, E.; Warren, M. J.; Chivers, P. T.; Robinson, N. J. Bacterial sensors define intracellular free energies for correct enzyme metalation. *Nat. Chem. Biol.* **2019**, *15*, 241−249.
(61) Hitomi, Y.; Outten, C. E.; O'Halloran, T. V. Extreme Zinc-binding thermodynamics of the metal sensor/regulator protein, ZntR. *J. Am. Chem. Soc.* **2001**, *123*, 8614−8615.
(62) Philips, S. J.; Canalizo-Hernandez, M.; Yildirim, I.; Schatz, G. C.; Mondragon, A.; O'Halloran, T. V. Allosteric transcriptional regulation via changes in the overall topology of the core promoter. *Science* **2015**, *349*, 877−881.
(63) Shi, W.; Zhang, B.; Jiang, Y.; Liu, C.; Zhou, W.; Chen, M.; Yang, Y.; Hu, Y.; Liu, B. Structural basis of copper-efflux-regulator-dependent transcription activation. *iScience* **2021**, *24*, 102449.
(64) Strausak, D.; Solioz, M. CopY is a copper-inducible repressor of the Enterococcus hirae copper ATPases. *J. Biol. Chem.* **1997**, *272*, 8932−8936.

https://doi.org/10.1021/acsomega.3c06336
ACS Omega 2023, 8, 39886−39895

(65) Portmann, R.; Poulsen, K. R.; Wimmer, R.; Solioz, M. CopY-like copper inducible repressors are putative 'winged helix' proteins. *BioMetals* **2006**, *19*, 61−70.
(66) Hofmann, L.; Ruthstein, S. EPR Spectroscopy Provides New Insights into Complex Biological Reaction Mechanisms. *J. Phys. Chem. B* **2022**, *126*, 7486−7494.
(67) Hofmann, L.; Mandato, A.; Saxena, S.; Ruthstein, S. The use of EPR spectroscopy to study transcription mechanisms. *Biophys. Rev.* **2022**, *14*, 1141−1159.
(68) Shenberger, Y.; Gevorkyan Airapetov, L.; Hirsch, M.; Hofmann, L.; Ruthstein, S. An in-cell spin-labelling methodology provides structural information on cytoplasmic proteins in bacteria. *Chem. Commun.* **2023**, *59*, 10524−10527.
(69) Shenberger, Y.; Gevorkyan-Airapetov, L.; Hirsch, M.; Hofmann, L.; Ruthstein, S. An in-cell spin-labelling methodology provides structural information on cytoplasmic proteins in bacteria. *Chem. Commun.* **2023**, *59*, 10524−10527.
(70) Yakobov, I.; Mandato, A.; Hofmann, L.; Singewald, K.; Shenberger, Y.; Gevorkyan-Airapetov, L.; Saxena, S.; Ruthstein, S. Allostery-driven changes in dynamics regulate the activation of bacterial copper transcription factor. *Protein Sci.* **2022**, *31*, No. e4309.
(71) Hirsch, M.; Hofmann, L.; Shenberger, Y.; Gevorkyan-Airapetov, L.; Ruthstein, S. Conformations and Local Dynamics of the CopY Metal Sensor Revealed by EPR Spectroscopy. *Biochemistry* **2023**, *62*, 797−807.
(72) Worswick, S. G.; Spencer, J. A.; Jeschke, G.; Kuprov, I. Deep neural network processing of DEER data. *Sci. Adv.* **2018**, *4*, No. eaat5218.

https://doi.org/10.1021/acsomega.3c06336
ACS Omega 2023, 8, 39886−39895